Crystallographic Study of Steps along the Reaction Pathway of D-Amino Acid Aminotransferase[†,‡]

Daniel Peisach,[§] David M. Chipman,[∥] Peter W. Van Ophem,[⊥] James M. Manning,[⊥] and Dagmar Ringe*[,#]

Program in Bioorganic Chemistry, Brandeis University, 415 South Street, Waltham, Massachusetts 02254-9110, Department of Life Sciences, Ben Gurion University, Beer-Sheva, 84105, Israel, Department of Biology, Northeastern University, Boston, Massachusetts 02215, and Departments of Biochemistry and Chemistry and Rosenstiel Basic Medical Sciences Research Center, Brandeis University, 415 South Street, Waltham, Massachusetts 02254-9110

Received November 25, 1997; Revised Manuscript Received January 26, 1998

ABSTRACT: The three-dimensional structures of two forms of the D-amino acid aminotransferase (D-aAT) from *Bacillus* sp. YM-1 have been determined crystallographically: the pyridoxal phosphate (PLP) form and a complex with the reduced analogue of the external aldimine, *N*-(5′-phosphopyridoxyl)-D-alanine (PPDA). Together with the previously reported pyridoxamine phosphate form of the enzyme [Sugio et al. (1995) *Biochemistry 34*, 9661], these structures allow us to describe the pathway of the enzymatic reaction in structural terms. A major determinant of the enzyme's stereospecificity for D-amino acids is a group of three residues (Tyr30, Arg98, and His100, with the latter two contributed by the neighboring subunit) forming four hydrogen bonds to the substrate α-carboxyl group. The replacement by hydrophobic groups of the homologous residues of the branched chain L-amino acid aminotransferase (which has a similar fold) could explain its opposite stereospecificity. As in L-aspartate aminotransferase (L-AspAT), the cofactor in D-aAT tilts (around its phosphate group and N1 as pivots) away from the catalytic lysine 145 and the protein face in the course of the reaction. Unlike L-AspAT, D-aAT shows no other significant conformational changes during the reaction.

D-Amino acid aminotransferase (D-aAT, EC 2.6.1.21) catalyzes transamination between various D-amino acids and their respective α-keto acids. The enzyme is vital for bacteria because it provides one important route for the synthesis of the essential bacterial cell wall components D-alanine and D-glutamate, as well as other D-amino acids (*1*). For this reason, it is a target enzyme for the development of novel antimicrobial agents.

The D-aAT from the thermophillic *Bacillus* species YM-1 is a dimer with an overall molecular mass of 65 kilodaltons; each monomer consists of 282 amino acid residues and requires 1 pyridoxal phosphate (PLP) molecule as cofactor (*2*). The crystal structure of D-aAT in the pyridoxamine (PMP) form has recently been solved at 1.94 Å resolution (*3*). D-aAT has no sequence similarity to the well-studied L-amino acid aminotransferases (*4*), but does have significant sequence identity to a bacterial branched-chain L-amino acid aminotransferase (BCAT, EC 2.6.1.42) and 4-amino-4-deoxychorismate lyase (28% and 23% identity, respectively, to the *Escherichia coli* enzymes). The structure also has a unique fold not seen for any other PLP-dependent enzyme, with the exception of the recently determined BCAT from *E. coli* (*5*).

The accepted pathway for transamination, characterized for a number of PLP-dependent enzymes, proceeds by a ping-pong kinetic mechanism, which consists of two half-reactions (Figure 1). The mechanism shown here is based primarily on kinetic and structural evidence obtained with L-aspartic acid aminotransferase (L-AspAT) (*6, 7*). The enzyme starts in the internal aldimine form, with a Schiff-base link between an active site lysine and the PLP. Upon binding of a substrate amino acid, a transaldimination reaction releases the lysine residue, and an external aldimine between substrate and PLP is formed. The lysine is the catalytic base in the next step, a 1,3 prototropic shift that converts the internal aldimine into a ketimine intermediate (*8*). The final step in the first half-reaction is the hydrolysis of the ketimine to form pyridoxamine phosphate (PMP) and an α-keto acid. The second half-reaction is the reversal of these steps with a different keto acid. On the basis of spectroscopic characterization, D-aAT seems to utilize a mechanism similar to that demonstrated for L-AspAT (*9*).

In addition to its substrate and product specificity for D-amino acids, the stereochemistry of the reaction catalyzed by D-aAT is different from that of L-AspAT and most other PLP-dependent enzymes in another important sense. Whereas most aminotransferases add or remove the *pro-S* hydrogen at C4A of the cofactor, D-aAT transfers the *pro-R* hydrogen (*10*). Somewhat surprisingly, it shares this property, as well as inverted (negative) Cotton effects in its circular dichroism spectrum at 420 nm (*9, 11*), with BCAT, an L-amino acid-

[†] This work was supported by a grant from the National Science Foundation and (in part) by a grant from the Lucille P. Markey Charitable Trust. D.P. was supported (in part) by a National Institutes of Health training grant.

[‡] Atomic coordinates are available from the Brookhaven Protein Data Bank under entry codes 3DAA and 4DAA.

* Address correspondence to this author at Brandeis University.

[§] Program in Bioorganic Chemistry, Brandeis University.

[∥] Ben Gurion University.

[⊥] Northeastern University.

[#] Departments of Biochemistry and Chemistry and Rosenstiel Basic Medical Sciences Research Center, Brandeis University.

S0006-2960(97)02884-5 CCC: $15.00
Published on Web 03/17/1998

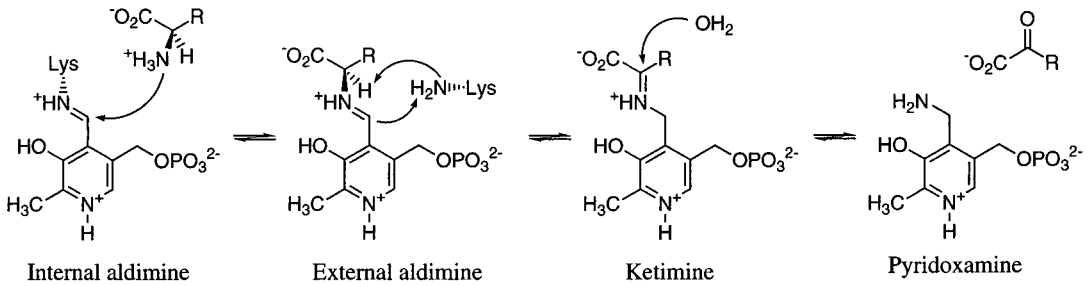

FIGURE 1: Reaction pathway for a transamination half-reaction of D-aAT, in which an amino acid is converted to the keto acid and the enzyme converted from the PLP to the PMP form. The completion of the catalytic cycle requires reversal of this reaction with a substrate keto acid.

specific aminotransferase. The crystal structure of the PMP form of D-aAT (D-aAT/PMP) explains the stereochemistry of this enzyme with regard to the cofactor (*3*). The PMP molecule is bound to D-aAT with its *re* side facing the protein (and the catalytic lysine 145), in contrast to what is observed with L-AspAT and other PLP-dependent enzymes, in which the *si* side of the coenzyme faces the protein. It has very recently been shown that the cofactor has the same orientation in BCAT as it does in D-aAT (*5*).

The crystal structure of the PMP form of D-aAT leaves two questions unanswered: What is the conformation of the cofactor in the internal aldimine form, and what groups in the active site determine the orientation of bound substrates, and thus specificity for D-amino acids? When the recombinant enzyme is isolated, the cofactor is found partly in the PLP and partly in the PMP form. To obtain a structure of the PLP form, it was necessary to convert all of the enzyme into this form with α-ketoglutarate before crystallization. The crystal structure of the PLP form of D-aAT (D-aAT/PLP) has now been solved at 2.4 Å resolution, and is reported here.

To establish the mode by which substrate binds to the active site, two types of experiments are possible. The ideal experiment would be to determine the structure of the substrate bound to the enzyme. However, D-aAT is catalytically competent in the crystalline state, and turns over any bound substrate. Alternatively, one can crystallize the complex between the enzyme and a noncovalent inhibitor. This method suffers from the drawback that such a structure could give ambiguous information about the movement of the cofactor. Consequently, another strategy is needed. The intermediates postulated for the reaction catalyzed by D-aAT are an external aldimine and a ketimine (Figure 1). One might mimic these intermediates by reducing the aldimine/ketimine double bond to a stable analogue. This strategy has been used successfully for L-AspAT (*6*, *12*, *13*). We now report the structure of such a reduced analogue, *N*-(5′-phosphopyridoxyl)-D-alanine (PPDA), bound to D-aAT (D-aAT/PPDA) at 1.9 Å resolution. The comparison of the active site structure of D-aAT with this analogue bound to that of the native PLP and PMP forms of the enzyme allows us to describe the reaction pathway for the enzyme in greater detail. We also discuss the similarities and differences between D-aAT and BCAT with regard to substrate specificity and stereoselectivity.

MATERIALS AND METHODS

All chemicals were the highest purity available from commercial sources.

Preparation of N-(5′-Phosphopyridoxyl)-D-alanine (PPDA). PPDA was synthesized by a modification of the method of Korytnyk et al. (*14*). Pyridoxal 5′-phosphate (271 mg, 1.0 mmol) and D-alanine (188 mg, 2.1 mmol) were dissolved in 10 mL of methanol and brought to a pH between 7 and 7.5 with 50% NaOH. The solution was stirred for 20 min at room temperature, and then $NaBH_4$ (187 mg, 4.9 mmol) was slowly added. After 15 min, concentrated HCl was added to bring the pH to about 3, and the methanol was evaporated on a vacuum rotary evaporator. The residue was dissolved in water, neutralized, and loaded on a 1.2 × 18 cm Dowex 1 × 8 column, which was eluted with 50 mL of water, followed by a gradient to 1 M acetic acid over 500 mL. Aliquots were monitored for absorbance at 325 nm. The tailing half of the peak which eluted was collected and evaporated to dryness under high vacuum. The product showed an absorbance maximum at 325 nm. The NMR spectrum showed peaks at 8.4 ppm (s, 1H), 5.3 ppm (d, 2H), 4.7 ppm (s, 2H), 4.25 ppm (q, 1H), 2.8 ppm (s, 3H), and 1.8 ppm (d, 3H). The spectrum also showed that the sample was contaminated with about 15 mol % of alanine.

Preparation of the Complex of D-aAT with PPDA. D-aAT (4 mg, 2 mg/mL) purified as previously described (*3*) was incubated with 5 mM phenylhydrazine in 0.5 mL of 70 mM potassium phosphate buffer, pH 7.2, for 50 min at 37 °C. The protein was separated from small molecules by gel filtration on a 2.7 × 10 cm Sephadex G50M column eluted with 10 mM potassium phosphate buffer, pH 8.0. Protein fractions were combined, and PPDA (2.5 μmol) was added. The protein was concentrated with a Centricon 10 membrane concentrator (Millipore Corp., Bedford, MA). Samples of the protein before and after addition of PPDA were assayed for the ability to be reactivated with PLP. PPDA addition blocked reactivation of D-aAT. Some basal transaminase activity was present before and after the addition of PPDA, probably due to residually bound PMP which did not react with phenylhydrazine.

Crystallizations. D-aAT was concentrated to 30 mg/mL in 100 mM potassium phosphate buffer, pH 7.6, containing 0.05 mM PLP and 0.01 mM β-mercaptoethanol. The protein was crystallized by the hanging drop method with 25% poly(ethylene glycol) (PEG) 4000, 200 mM ammonium sulfate, 100 mM sodium acetate, pH 4.6, and 1 mM α-ketoglutarate. Two microliters of protein solution was mixed with 2 μL of the above crystallization solution and suspended at room temperature over 0.5 mL of the crystallization solution. After 2 weeks, this gave rise to a single yellow crystal (due to the presence of an internal aldimine) of D-aAT in the PLP form with dimensions 1.1 × 0.6 × 0.5 mm^3, which was used for data collection.

The PPDA complex was similarly crystallized, except that the crystallization solution contained 26−28% PEG 4000, 300 mM sodium acetate, and 100 mM Tris−chloride buffer, pH 8.5. Heterogeneous microseeding with crushed crystals of native D-aAT in the PLP form, grown under the same Tris buffer conditions, gave rise within 2 days to colorless plate-shaped crystals that continued to grow for a week. The crystals were small and thin. One crystal with dimensions $0.2 \times 0.2 \times 0.05$ mm^3 was transferred into cryoprotecting oil (available from Håkon Hope, Department of Chemistry, U. C. Davis) and flash-cooled in a stream of gaseous nitrogen at 100 K and used for data collection.

The crystal of the PLP form of D-aAT belongs to the monoclinic space group *C2*. The unit cell parameters are $a = 141.1$ Å, $b = 68.9$ Å, $c = 84.4$ Å, and $\beta = 119.5°$, which corresponds to a unit cell volume of 715 000 Å^3. The volume per unit mass (V_m) calculated with the assumption that there is one dimer (65 000 daltons) per asymmetric unit is 2.7 Å^3/Da, which is in the range of 1.6−3.6 Å^3/Da typical for protein crystals (*15*).

The crystals of D-aAT complexed with PPDA belong to the orthorhombic space group $P2_12_12_1$. Its unit cell parameters are $a = 77.1$ Å, $b = 78.3$ Å, and $c = 88.4$ Å, which corresponds to a unit cell volume of 533 000 Å^3. The volume per unit mass (V_m) calculated with the assumption that there is one dimer per asymmetric unit is 2.1 Å^3/Da, which is also in the range typical for protein crystals.

Solution of the Crystal Structure. Data for the PLP crystal form were collected at 4 °C with a scan width of 1° per frame and an exposure time of 15 min per frame on a RAXIS IIC image plate system mounted on a Rigaku RU-200B X-ray generator running at 45 kV and 140 mA. The data set was collected from a single crystal, and was 91.4% complete to 2.25 Å resolution. Frames were integrated and scaled together using the HKL package (DENZO and SCALEPACK) from Molecular Structures Corp. (Table 1).

X-ray diffraction data for the PPDA complex were collected at the National Synchrotron Light Source at Brookhaven National Laboratories on beamline X12C using a MAR image plate detector. Data were collected from a single crystal at 100 K, with a scan width of 1° per frame and an exposure time of 30 s per frame. The data set was 87.1% complete to 1.80 Å resolution. Frames were integrated and scaled together using the HKL package (Table 1).

Both structures were solved by molecular replacement using the native monoclinic structure of the PMP form of D-aAT (*3*) as search probe in the program AMORE, which is part of the CCP4 package (*16*). The program XPLOR (*17, 18*) was then used for all remaining refinement. The program O (*19*) was used for examination and manual adjustment of the structure during refinement. Rigid body refinement (of each monomer of the asymmetric unit) was first performed to optimize the initial location of the two monomers. A solvent mask was calculated to better approximate the low-resolution data. This was followed by several cycles of positional refinement, grouped temperature factor refinement, placement of water molecules, and finally individual temperature factor refinement.

Water molecules were located with PEAKMAX and WATPEAK from the CCP4 package (*20*). Only 79 water molecules were modeled into the structure of the PLP form of D-aAT. However, electron density for several water molecules was clearly seen in the active site. In addition, there is a region of electron density close to arginine 98*, histidine 100*, and tyrosine 31 that is too large to be accounted for by a water molecule. (Figure 2; the asterisk denotes a residue from the other monomer in the homodimer.) After some consideration, this was modeled as a sulfate ion because the sulfate ion concentration was twice that of phosphate ion or acetate ion in the crystallization solution. However, we cannot rule out a mixture of any of these ions. Crystallographically, we cannot determine the orientation of histidine 100* directly. In the PPDA structure, the side chain of His100* is close to two water molecules and the carboxylate end of PPDA. WAT675 is observed in every structure of D-aAT other than the PLP form (*3, 21*). We chose the orientation reported here because in this orientation both nitrogens of the histidine side chain make hydrogen bonding interactions (2.6 Å to WAT824 and 3.0 Å to WAT675). As a consequence, the carboxylate of PPDA is within 3.3 Å of atom CE of the histidine. This may be an example of a weak C−H···O interaction (*22*).

Figures 2, 3, 5, and 6 were created from coordinate files with the program MOLSCRIPT (*23*).

Table 1: Data Collection and Refinement

protein	PLP form	PPDA complex
Crystal Data		
space group	*C2*	$P2_12_12_1$
unit cell parameters		
a (Å)	141.1	77.1
b (Å)	68.9	78.3
c (Å)	87.4	88.4
β (deg)	119.5	90.0
Data Collection		
reflections, observed	92975	57553
reflections, unique	31959	43764
R_{sym} (% on *I*)	14.9	6.2
resolution (Å)	30−2.25	30−1.80
I/σ (*I*) cutoff	>0	>0
completeness, overall (%)	91.4	87.1
highest resolution shell (Å)	2.5−2.25	1.85−1.80
completeness, highest resolution (%)	69.5	76.1
Refinement		
resolution (Å)	30−2.4	30−1.90
I/σ (*I*) cutoff	>0	>0
reflections	29294	36837
R-factor	18.0	19.6
R-free	24.6	24.3
protein atoms	4466	4466
cofactor atoms	30	42
sulfate atoms	10	0
water molecules	79	252
B-factor model	individual	individual
restraints (rms observed)		
bond length (Å)	0.007	0.008
bond angles (deg)	1.2	1.2
improper angles (deg)	1.1	1.2
dihedral angles (deg)	24.0	23.9

RESULTS AND DISCUSSION

The reaction catalyzed by D-aAT involves the conversion of an amino acid to a keto acid. In the process, the essential cofactor, pyridoxal phosphate, is converted from the aldehyde form (PLP), which occurs as an internal aldimine on the enzyme, to the amine form (PMP) (Figure 1). The crystal structure of D-aAT in the PMP form (D-aAT/PMP) has

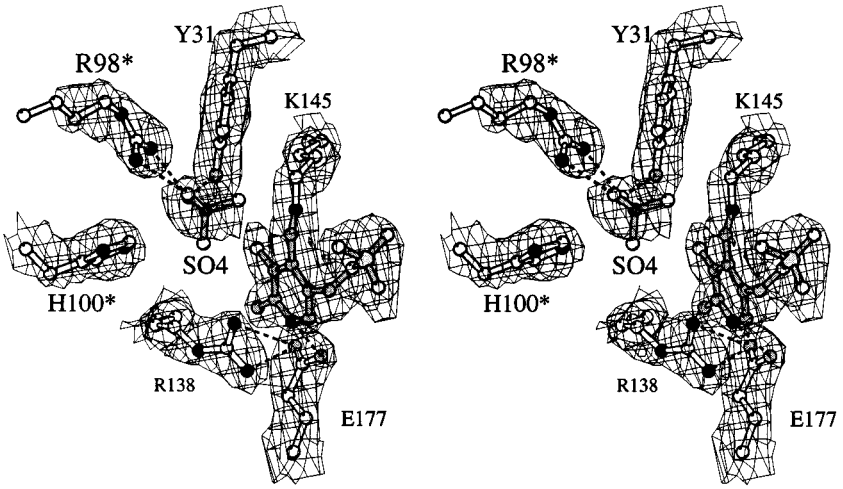

FIGURE 2: Stereoview of the electron density in the region of the active site of the PLP form of D-aAT. Electron density shown is a $2F_o - F_c$ map drawn at a 1.0 sigma contour. A sulfate ion has been modeled into the electron density near the carboxylate binding "trap" of the protein. Solvent access to the site is from the viewer's direction.

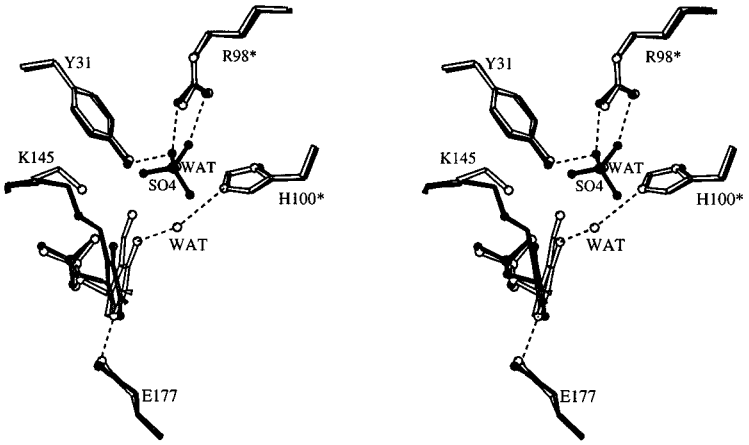

FIGURE 3: Stereo comparison between the structure of the active site of D-aAT in the PLP form (dark bonds) and that in the PMP form (light bonds). This view places the solvent on the right. The sulfate ion is observed in the PLP form of the enzyme, whereas in the PMP form there seems to be a water molecule at this position. Note that in the PLP form, the cofactor is tilted by ~25° toward the protein (to the left) relative to its position in the PMP form, due to the covalent bond to Lys145. Dashed lines indicate distances of less than 3.2 Å.

previously been reported (*3*). We have now solved the crystal structures of D-aAT in the PLP form (D-aAT/PLP) and of D-aAT complexed with PPDA, an analogue of both the external aldimine and ketimine intermediates (D-aAT/PPDA). The latter structure defines the conformation of bound substrate, which determines the substrate stereospecificity of the enzyme. We can now describe the course of the reaction catalyzed by D-aAT in structural terms, on the basis of the three structures.

The PLP Form of the Enzyme. The structure of D-aAT/PLP was solved to 2.4 Å resolution (Table 1). Although this form was crystallized under different conditions and in a different space group than that of the previously determined D-aAT/PMP, the overall structure of the protein is almost identical to that of the native enzyme in the PMP form (rms deviation on α carbons, 0.57 Å). Neither the relative positions of the two domains in a subunit nor the monomer−monomer interactions in the dimer are different. There are small differences in a few surface loops of the protein. These differences can be due to changes in crystal packing and do not seem to be relevant to the chemical properties of the active site. It should be noted that in all three of these structures, the C-terminal amino acids 278−282 are not seen in the electron density, probably because of disorder. A surface loop including residues 104−106 is also disordered, and is observed clearly only in the PPDA structure.

The major structural differences between the PLP and PMP forms of D-aAT lie in the active site region (Figure 3). The cofactor is held in place in the active site of D-aAT by numerous noncovalent interactions, such that the *si* face of the pyridine ring is toward the solvent and incoming substrates, and the other side (*re*) faces the protein. Although the PLP form of the enzyme has an aldimine linkage between the cofactor and lysine 145, many of the other interactions between the cofactor and D-aAT are unchanged on going from one form of the enzyme to another (Figure 4). Of these, the strongest anchor holding the cofactor to the protein involves interactions between the phosphate moiety and side chain and backbone atoms of the protein. Two waters are observed at hydrogen bonding distance to cofactor phosphate oxygens in D-aAT/PLP which had not been observed in D-aAT/PMP. The pyridine nitrogen (N1; see Figures 4 and 7 for atom naming scheme used) is held in place by Glu177, which is in turn held by a salt bridge with Arg138. Neither the phosphate nor the N1 nitrogen have changed their positions in the PLP form relative to those in the PMP form of the enzyme.

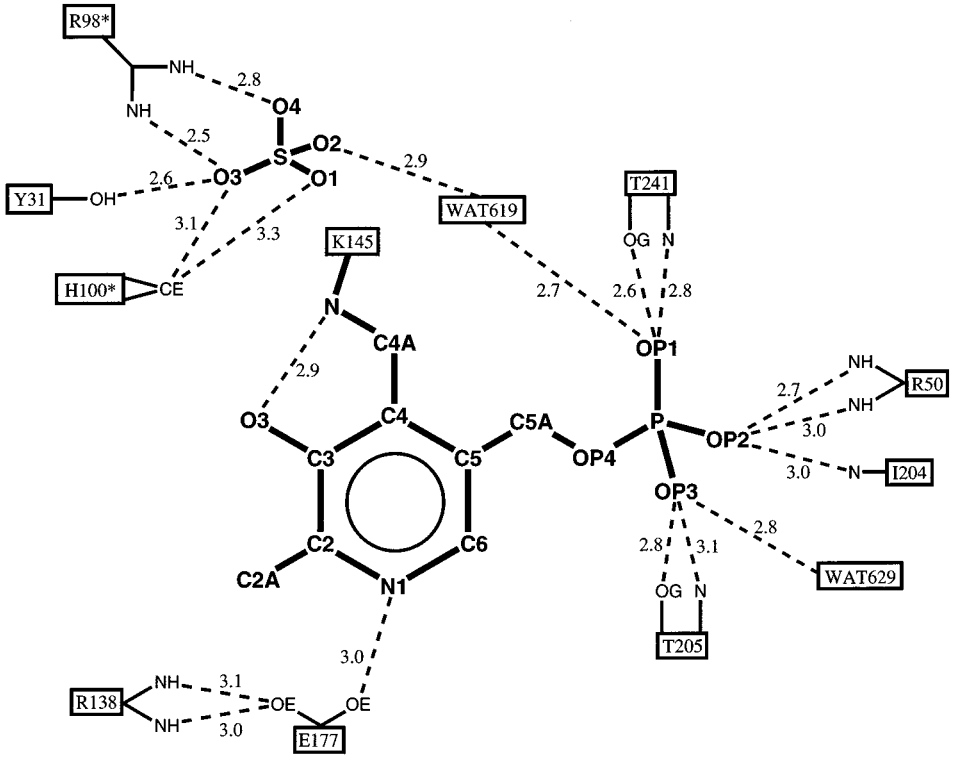

FIGURE 4: Schematic diagram showing the bound cofactor and its surroundings in the PLP form of D-aAT. Atom names are given by PDB convention. Hydrogen bonding distances are given for interactions less than 3.5 Å.

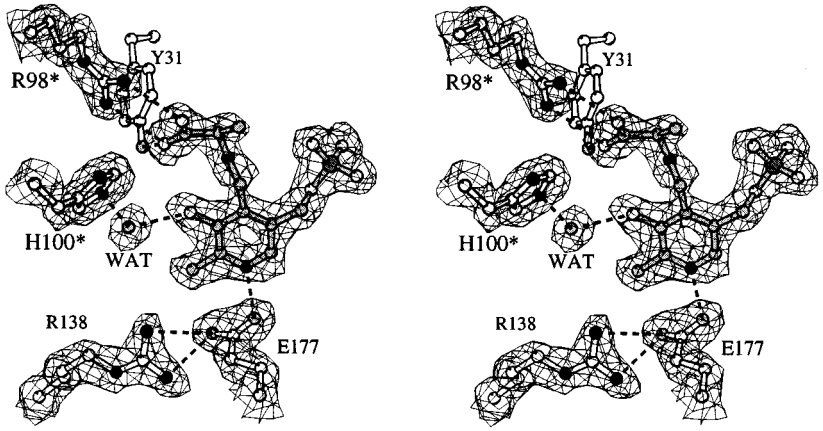

FIGURE 5: Stereoview of the electron density in the region of the active site of the complex of D-aAT with PPDA. Electron density shown is an unbiased simulated annealing $2F_o - F_c$ omit map drawn at a 1.0 sigma contour. All atoms in PPDA were left out of the model for this map. The density for Tyr31 was left out of this picture for clarity. The view is similar to that in Figure 2.

On the other hand, in the PLP form of the enzyme the cofactor is tilted as a unit toward the protein about an axis defined by the phosphate group and the N1 nitrogen. This tilt rotates the cofactor by 25° relative to its position in the PMP form. A similar movement of the cofactor about this same axis has been observed in complexes of L-AspAT (*6*, *24*). The effect of this tilt is that atom C4A moves by 1.5 Å and a number of interactions between the cofactor and protein change. To make the internal aldimine with the cofactor, the NZ nitrogen of the side chain of lysine 145 moves toward the solvent by 0.6 Å from its location in the PMP form of the enzyme (Figure 3). The environment of the phenolic oxygen (O3) in D-aAT/PLP is also different than that in D-aAT/PMP. For example, the bound water molecule observed between this oxygen, His100* and a backbone carbonyl in the PMP form, the PPDA complex, and cycloserine complex (*21*) is not seen in the PLP form of the enzyme. This may be due to the difference in resolution between these two structures.

A feature of electron density that we interpret as a sulfate ion is observed near the cofactor in the D-aAT/PLP structure (Figure 2). This sulfate ion interacts with residues from both subunits of the homodimer. These include Tyr31 from the monomer to which the cofactor is bound, and Arg98* from the other monomer. His100* is somewhat further from the sulfate. Arg98* had been proposed as the residue that interacts with the carboxylate of the incoming substrate (*3*). This sulfate is indeed in the position of the substrate carboxylate seen in the PPDA structure (see below). Bridging between the sulfate ion and the phosphate group of the cofactor is WAT619, which was not seen in the D-aAT/PMP structure; it is possible that this bridging interaction orders this water molecule.

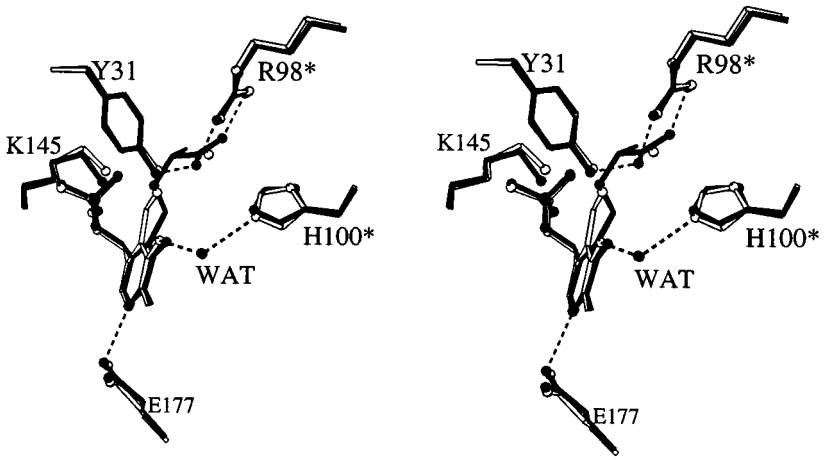

FIGURE 6: Structural comparison between the active site of D-aAT with the analogue PPDA bound (dark bonds) with that of the enzyme in the PMP form (light bonds). Note that the cofactor has essentially the same tilt in both structures. Dashed lines indicate distances of less than 3.2 Å.

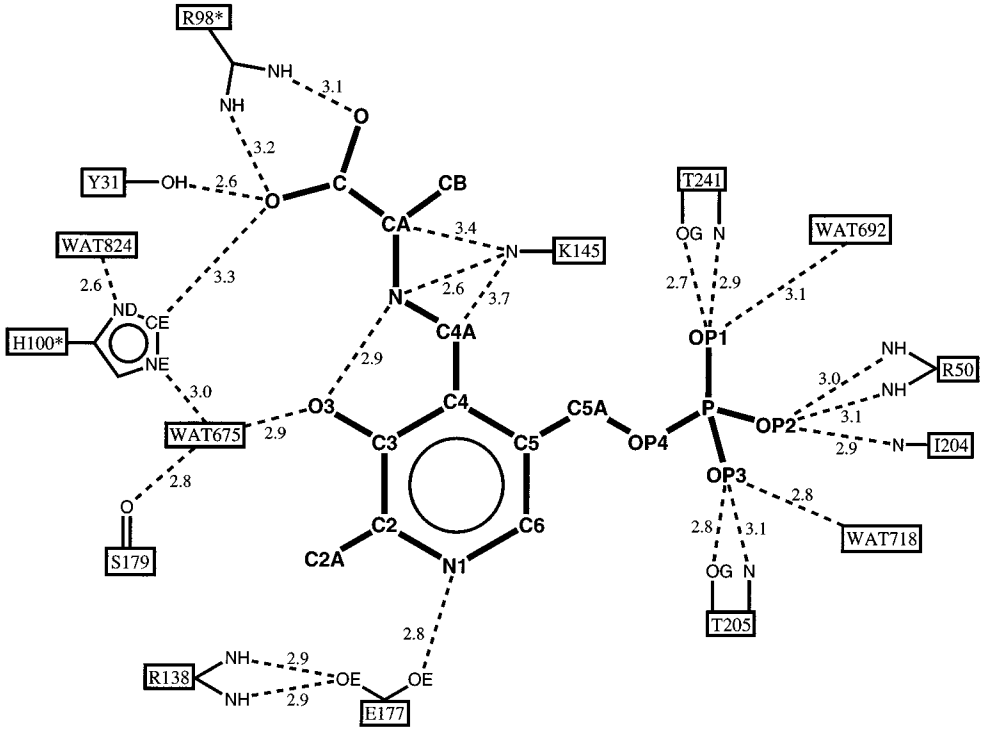

FIGURE 7: Schematic diagram showing the polar interactions between bound PPDA and the active site of D-aAT.

The PPDA Form of the Enzyme. The structure of the enzyme complexed with PPDA, a reduced analogue of the aldimine and ketimine forms of the cofactor−substrate complex, was solved to 1.9 Å resolution. Despite the fact that this form of the enzyme was crystallized in yet a third set of chemical conditions and in yet another space group, the protein structure remains essentially unchanged except for the active site region. The rms deviation between α carbon positions in D-aAT/PPDA and D-aAT/PLP is 0.42 Å. There is no evidence for a conformational change to close the active site upon substrate binding, as is observed for L-AspATs (*6*, *24*−*26*).

The electron density due to PPDA in the active site (Figure 5) can be interpreted in an unambiguous manner. The pyridine ring is in the expected region of the active site and has a well-defined shape, and the amino acid analogue portion of the molecule is covalently attached and has an asymmetric shape so there is no question of its orientation. The position of the cofactor portion of PPDA is similar to that of the cofactor in D-aAT/PMP (Figure 6), but it has tilted even further from its position in D-aAT/PLP. In D-aAT/PPDA, atom C4A is 2.0 Å from its position in the PLP form of the enzyme, tilting the cofactor by about 35°. The cofactor phosphate group and N1 atom form essentially the same interactions with the protein as they do in the PLP and PMP forms (Figure 7). WAT718 is in essentially the same position as WAT629 of the PLP form of the enzyme.

The carboxylate of the covalently attached substrate moiety makes a number of interactions with the enzyme. It forms a bidentate salt-bridge with Arg98*, and one of its oxygens also interacts with His100* and Tyr31. These three residues make up a "carboxylate trap" which, together with the bound cofactor, must define the position and orientation of substrate binding. The positioning of the bound substrate relative to the catalytic base lysine 145 in turn defines substrate and product stereospecificity; only a D-amino acid would have

its α-proton pointing toward the catalytic base. The side chain of the substrate points into a large pocket, which would account for the ability of this enzyme to accommodate a wide variety of D-amino acid substrates (*27*).

The catalytic base Lys145 is close to the position it has in the PMP form of the enzyme. Atom NZ is 2.6 Å away from atom N of PPDA, and almost equidistant from atoms C4A and CA (3.7 and 3.4 Å, respectively). This atom also appears to interact with the hydroxyl group of Tyr31, either directly (it is 3.6 Å away) or through a bridging water molecule (Figure 7). As Tyr31 also interacts with the substrate carboxylate, this interaction may raise the pK_a of Lys145 when a substrate is bound. Although there are no direct interactions between the protein and the phenolic oxygen (O3) of the cofactor in this complex, an ordered water molecule (WAT675 in DaAT/PPDA) is observed within hydrogen bonding distance of this atom in all the crystal structures of D-aAT, except the PLP form. This water forms a polar contact with His100* and the backbone carbonyl of Ser195.

It is interesting to note that the structure of the derivative formed when the PLP form of D-aAT is irreversibly inhibited by the antibiotic D-cycloserine shares many features with the PPDA complex (*21*). In particular, the derivative formed between cycloserine and pyridoxal phosphate makes close polar contacts with the three groups of the "carboxylate trap", has a similar tilt of the pyridine ring, and has ordered water molecules bound to O3. It also shows no significant domain movements or closure of the active site. This strengthens the likelihood that the lack of a conformational change in D-aAT is a real property of its substrate binding.

The Reaction Pathway. The half-reaction of D-aAT with D-alanine to form pyruvate and the PMP form of the enzyme can be described in terms of the three structures compared here (Figure 8). The reaction of the PLP form of the enzyme is initiated by a nucleophilic attack of the α-amino group of D-alanine on C4A of the internal aldimine. The carboxylate trap (Arg98*, His100*, and Tyr31) must play an important role in positioning the incoming substrate for this reaction. Although we cannot define protein interactions with the *β*-carbon of D-alanine, it would appear that an L-amino acid would be too sterically restricted to be a good inhibitor as an abortive substrate. On the other hand, there is a pocket, whose entrance is defined by a loop from Ser240 to Ser243 (*3*), which could accommodate the wide range of D-amino acid substrates that react with D-aAT (*27*).

The eventual transfer of protons implied in step I (Figure 8; loss of a proton of the amino nitrogen and protonation of NZ of Lys145) may be mediated by the water molecules bound in the active site. Elimination of NZ of Lys145 from the tetrahedral intermediate leads to the external aldimine (step II). In contrast to L-AspAT (*6*), the formation of the external aldimine in D-aAT does not appear to be accompanied by any significant rearrangement of the protein, closure of the active site, or change in exposure to the solvent. Rather, the cofactor pivots outward from the protein by about 35°, around an axis loosely defined by anchors at atom N1 of the pyridine ring and the phosphate group.

Lys145 is now in a position to act as a general base/acid and catalyze the tautomerization of the external aldimine to the ketimine by removing the proton from the α-carbon of the amino acid and donating it to C4A of the cofactor, either sequentially (steps III and IV) or simultaneously. The freedom of the cofactor to rock slightly toward and away from the protein face, and the flexibility of the lysine side chain, should allow close approach of the side chain nitrogen to either carbon atom from a stereoelectronically preferred direction. A putative intermediate quinonoid form of the cofactor could be stabilized by the presumed protonation of N1, induced by its interaction with Glu177. The anchoring of the cofactor aldimine/ketimine intermediates by the substrate carboxylate trap, phosphate binding pocket, and Glu177, together with the position of Lys145, determines the strict stereospecificity of these proton transfers on the *si* face of the conjugated system.

The final steps of the reaction involve hydrolysis of the ketimine. We assume that the water attacks from the solvent side of the cofactor, although we cannot identify an ordered water molecule in, e.g., the PPDA complex as occupying the position of the attacking molecule. A base(s) responsible for removal of the protons from the atom that becomes the carbonyl oxygen of pyruvate cannot be identified. However, Lys145 is once again in a position to transfer protons to the nitrogen that will become the amino group of PMP. A network of water molecules hydrogen bonded to Tyr31 and/or O3 of the cofactor cannot be ruled out as participating in these proton transfers.

The half-reaction described in Figure 8 is reversible; the reversal of these steps with a different keto acid completes the catalytic cycle of the enzyme.

Comparison with the BCAT. BCAT from *E. coli* shares with D-aAT significant sequence identity, stereospecificity for *si* face addition of hydrogen to PLP (*10*), and a similar overall fold (*5*). Despite these similarities, BCAT is an aminotransferase specific for L-amino acids. A comparison of the crystallographic structures of BCAT (*5*) and D-aAT is instructive. The α-carbons of D-aAT and of one dimer from the hexameric crystallographic structure of BCAT can be superimposed with an rms deviation of 1.4 Å. Most of the key groups of residues that interact with the cofactors in the active sites of the two enzymes are conserved in the sequence and in the structures of the two enzymes (Figure 9): the catalytic Lys145 (159 in BCAT), Glu177 (193), and the residues that position the phosphate group, Arg50 (59), Thr205 (221), and Thr241 (257).

On the other hand, all the polar residues in D-aAT that comprise the "carboxylate trap" responsible for positioning the α-carboxyl group of a substrate are replaced by nonpolar residues in BCAT: Tyr31 by Phe36, His100 by Val109, and Arg98 by Met107 (which has a very different side chain conformation). The replacement of Tyr31 of D-aAT with Phe in BCAT raises a question about the importance of its (indirect) interaction with the phenolic oxygen of PLP for stabilization of intermediates along the reaction pathway. However, another replacement (of Leu140 by Tyr164 in BCAT) provides such an interaction with the phenolic oxygen of the cofactor. The side chains of Phe36 and Val109 of BCAT, together with others, form a large relatively hydrophobic pocket, which is appropriate for binding of the side chain of a branched-chain amino acid. An amino acid substrate of BCAT would thus bind with its side chain away from the phosphate of the cofactor, and its α-carboxyl group toward the C5 (phosphate) side of the cofactor. Since the catalytic lysine 159 is on the *re* side of the cofactor, this

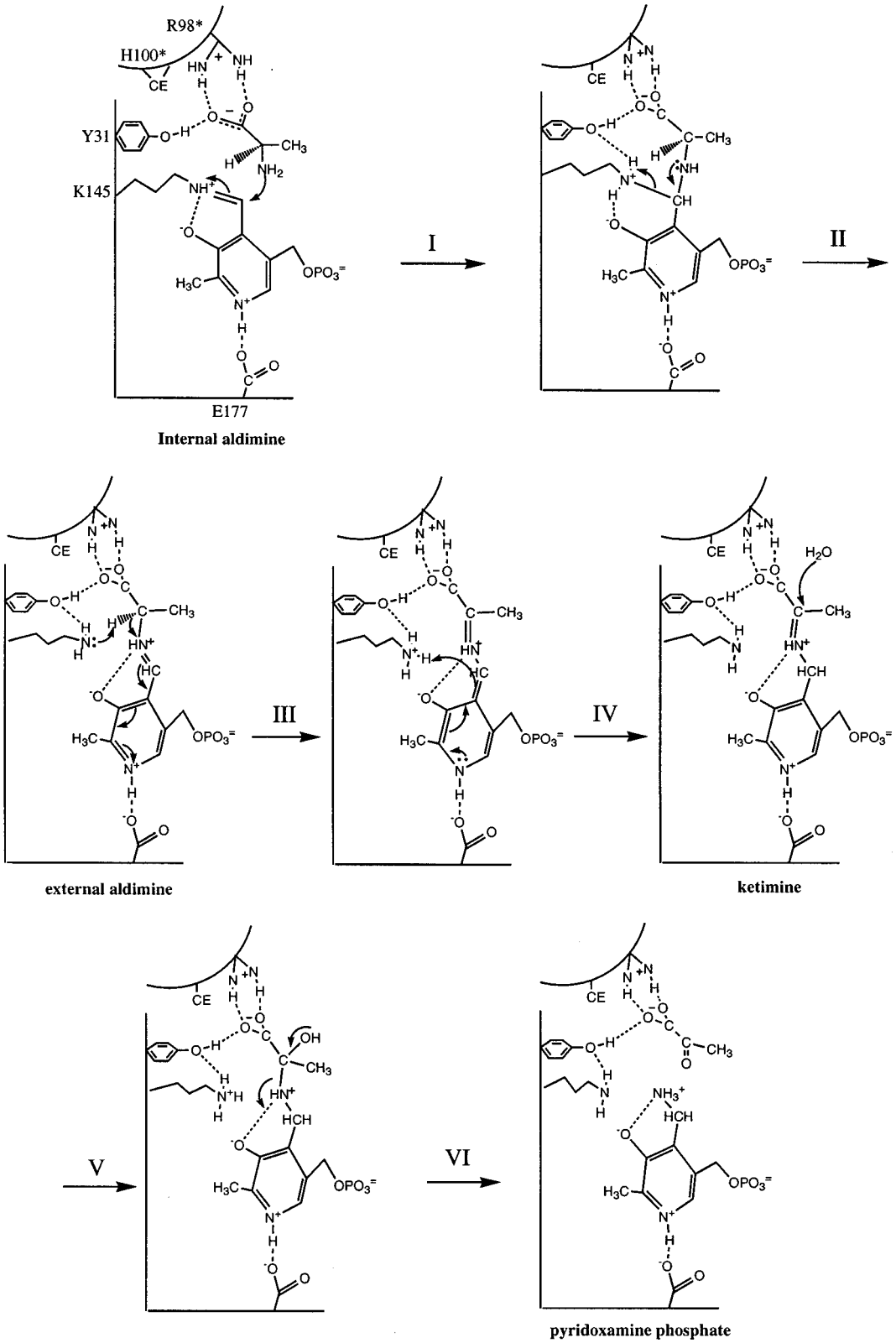

FIGURE 8: Proposed mechanism for one half-reaction of D-aAT. The steps shown are the conversion of the internal aldimine (PLP form of the enzyme) and an amino acid to the external aldimine (I and II), the tautomerization of the aldimine to the ketimine (III and IV), and the hydrolysis of the ketimine to the PMP form of the enzyme and a keto acid. The change in position of the pyridine ring in these illustrations is intended to reflect the rocking movement of the cofactor in the course of the reaction. Dashed lines indicate distances less than 3.2 Å based on distances observed in D-aAT/PPDA.

leads to specificity for transamination of L-amino acids. It is not clear what residue(s) in BCAT interact(s) with the substrate α-carboxyl group. It is conceivable that side chain rearrangements on substrate binding allow Arg40 to play this role; alternatively, an uncharged polar side chain and main chain NH groups could bind the carboxyl (*5*). This arrangement of the substrate relative to the cofactor is interesting: BCAT is the only PLP-dependent enzyme known in which

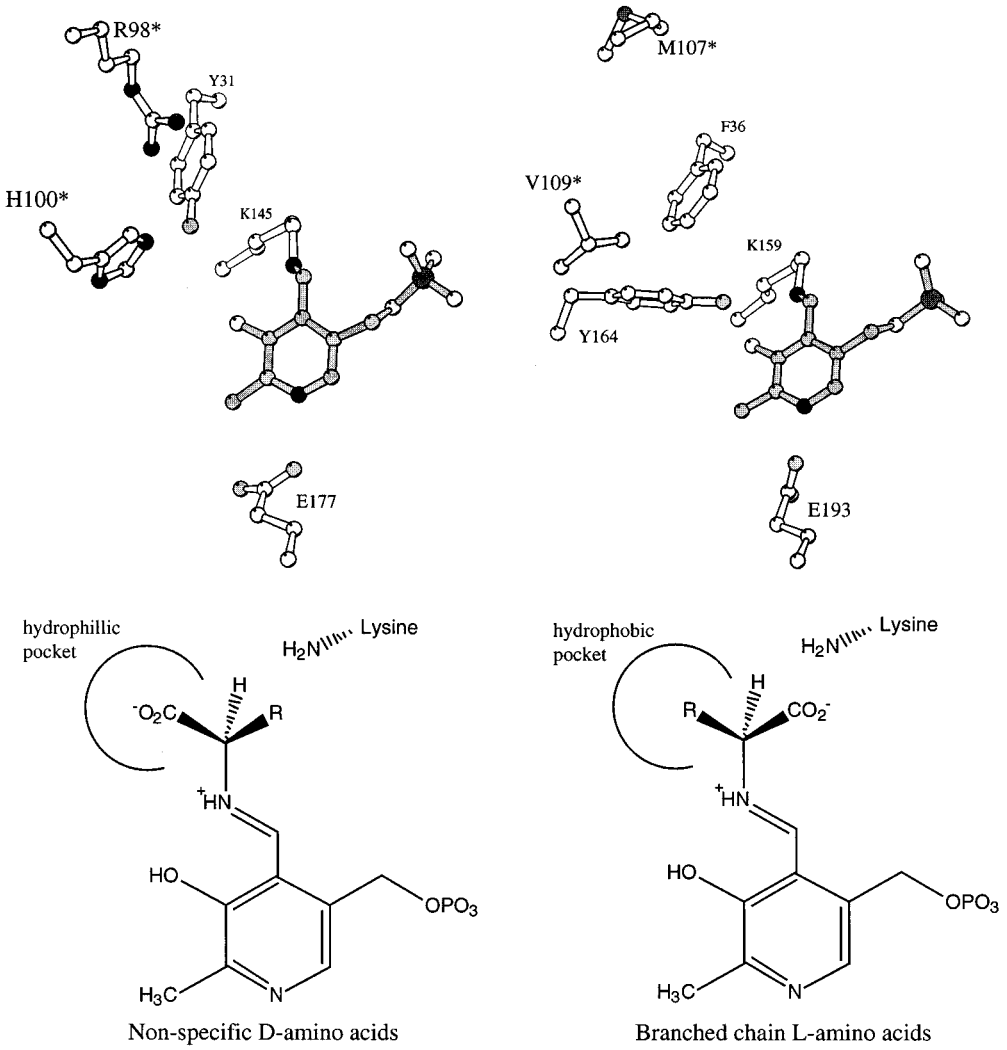

FIGURE 9: Comparison of the active sites of D-aAT (on left) and BCAT (on right) in the PLP form (top). Below are models of the external aldimine configurations of D-aAT and BCAT. The hydrophilic pocket interacts with the carboxylate of a substrate, which in turn positions the α-proton of only a D-amino acid toward the active site lysine. In BCAT, this pocket is hydrophobic. Assuming that this pocket now interacts with a hydrophobic side chain of an incoming amino acid, only a L-amino acid would have its proton pointing toward the active site lysine.

an α-amino acid is bound with its carboxyl group on the same side as the phosphate group.

Conclusions. D-aAT carries out specific transamination reactions by using the special properties of its cofactor PLP and some of the same catalytic residues employed by the well-characterized L-AspATs: a catalytic lysine as general base/acid and a carboxylic acid group associating with the N1 atom of the cofactor pyridine ring to ensure its protonation. Since the overall structural fold and sequence of D-aAT seem completely unrelated to L-AspAT, these features of D-aAT are no doubt the result of convergent evolution. The mechanistic convergence is incomplete, however, and D-aAT has some unique features. Although the conformations of the covalent substrate−cofactor intermediates are presumably similar for L-AspAT and D-aAT, the relation between the cofactor and the protein surface is reversed, leading to reversed stereochemistry of hydrogen transfer. Unlike L-AspAT, D-aAT is a relatively nonspecific aminotransferase. The position of the substrate α-carboxyl group in D-aAT is well fixed by several hydrogen bonds, while the side chain of the substrate is less firmly positioned. An important residue in the carboxylate binding site, Arg98*, is contributed by a loop from the neighboring subunit of the homodimer. Since the relative orientations of cofactor and protein are the same in BCAT as they are in D-aAT, there is only one possible explanation for the reversed substrate specificity observed with BCAT: the substrate must bind in the active site in the opposite orientation, which is made possible by changing the hydrophilic carboxylate trap pocket into a hydrophobic side chain pocket.

The new crystal structures reported here show that D-aAT exhibits the same sort of rocking motion of the cofactor in the course of its catalytic cycle as does L-AspAT; conversion of the internal aldimine to the external aldimine or ketimine is accompanied by a movement of C4A of the cofactor by about 1.5 Å. It does not appear, though, that D-aAT undergoes any significant domain motions that alter the exposure of the substrates or cofactor to the solvent.

ACKNOWLEDGMENT

We are grateful to Prof. Ken Hirotsu and to Kengo Okada for providing the coordinates of the branched-chain aminotransferase before their release to the PDB and to Prof. G. A. Petsko for his helpful discussions.

REFERENCES

1. Soda, K., and Esaki, S. (1985) in *Transaminases* (Christen, P., and Metzler, D. E., Eds.) pp 463−469, Wiley and Sons, New York.
2. Tanizawa, K., Masu, Y., Asano, S., Tanaka, H., and Soda, K. (1989) *J. Biol. Chem. 264*, 2445−2449.
3. Sugio, S., Petsko, G. A., Manning, J. M., Soda, K., and Ringe, D. (1995) *Biochemistry 34*, 9661−9669.
4. Tanizawa, K., Asano, S., Masu, Y., Kuramitsu, S., Kagamiyama, H., Tanaka, H., and Soda, K. (1989) *J. Biol. Chem. 264*, 2450−2454.
5. Okada, K., Hirotsu, K., Sato, M., Hayashi, H., and Kagamiyama, H. (1997) *J. Biochem. (Tokyo) 121*, 637−641.
6. Kirsch, J. F., Eichele, G., Ford, G. C., Vincent, M. G., Jansonius, J. N., Gehring, H., and Christen, P. (1984) *J. Mol. Biol. 174*, 497−525.
7. Malashkevich, V. N., Toney, M. D., and Jansonius, J. N. (1993) *Biochemistry 32*, 13451−13462.
8. Toney, M. D., and Kirsch, J. F. (1993) *Biochemistry 32*, 1471−1479.
9. Martinez Del Pozo, A., Merola, M., Ueno, H., Manning, J. M., Tanizawa, K., Nishimura, K., Asano, S., Tanaka, H., Soda, K., Ringe, D., and Petsko, G. A. (1989) *Biochemistry 28*, 510−516.
10. Yoshimura, T., Nishimura, K., and Ito, J. (1993) *J. Am. Chem. Soc. 115*, 3897−3900.
11. Yonaha, K., Misono, H., Yamamoto, T., and Soda, K. (1975) *J. Biol. Chem. 250*, 6983−6989.
12. Izard, T., Fol, B., Pauptit, R. A., and Jansonius, J. N. (1990) *J. Mol. Biol 215*, 341−344.
13. Malashkevich, V. N., Jager, J., and Ziak, M. (1995) *Biochemistry 34*, 405−414.
14. Korytnyk, W., and Paul, B. (1970) *J. Med. Chem. 13*, 187−191.
15. Matthews, B. W. (1968) *J. Mol. Biol. 33*, 491−497.
16. Navaza, J. (1990) *Acta Crystallogr. A46*, 619−620.
17. Brünger, A. T., Karplus, M., and Petsko, G. A. (1989) *Acta Crystallogr. A45*, 50−61.
18. Brünger, A. T., Kuriyan, J., and Karplus, M. (1987) *Science 235*, 458−460.
19. Jones, T. A., Zhou, J.-Y., and Cowan, S. W. (1991) *Acta Crystallogr. A47*, 110−119.
20. Navaza, J. (1994) *Acta Crystallogr. D50*, 760−763.
21. Peisach, D., Chipman, D. M., Van Ophem, P. W., Manning, J. M., and Ringe, D. (1998) *J. Am. Chem. Soc. 120*, 2268−2274.
22. Derewenda, Z. S., Lee, L., and Derewenda, U. (1995) *J. Mol. Biol. 252*, 248−262.
23. Kraulis, P. J. (1991) *J. Appl. Crystallogr. 24*, 946−950.
24. McPhalen, C. A., Vincent, M. G., and Jansonius, J. N. (1992) *J. Mol. Biol. 225*, 495−517.
25. Jager, J., Moser, M., Sauder, U., and Jansonius, J. N. (1994) *J. Mol. Biol. 239*, 285−305.
26. Picot, D., Sandmeier, E., Thaller, C., Vincent, M. G., Christen, P., and Jansonius, J. N. (1991) *Eur. J. Biochem. 196*, 329−341.
27. Bhatia, M. B., Martinez del Pozo, A., Ringe, D., Yoshimura, T., Soda, K., and Manning, J. M. (1993) *J. Biol. Chem. 268*, 17687−17694.

BI972884D